

CrossMark
click for updatesCite this: *J. Mater. Chem. A*, 2014, 2,
17463

Synthesis of novel platinum complex core as a selective Ag⁺ sensor and its H-bonded tetrads self-assembled with triarylamine dendrimers for electron/energy transfers†

Muthaiah Shellaiah, Mandapati V. Ramakrishnam Raju, Ashutosh Singh,
Hsin-Chieh Lin, Kung-Hwa Wei and Hong-Cheu Lin*

A novel platinum complex PtC with a tri-armed uracil hydrogen-bonded (H-bonded) unit was synthesized via a modular synthetic approach and characterized by ¹H, ¹³C NMR and MALDI-TOF mass spectroscopies. Two H-bonded tetrads, PtC-(TPAD1)₃ and PtC-(TPAD2)₃, based on a metal core PtC complexed with two generations of triarylamine dendrimers, TPAD1 and TPAD2 (with electron-donating nature), were successfully constructed with improved organic solubility via a classical H-bonded self-assembly approach. Supramolecular H-bonding in solution and solid state was elucidated by ¹H NMR titrations, IR spectral studies and time resolved photoluminescence (TRPL) measurements. The electron/energy transfers, as well as the self-assemblies of supramolecular tetrads, were established by UV-Vis and PL titrations and AFM morphological studies. Furthermore, metal complex core PtC showed selective sensitivity towards Ag⁺ ions through fluorescence turn-off responses without any interference from other common metal ions. The 1 : 1 binding stoichiometry and complexation mechanism between the probe and Ag⁺ ion was established by ¹H NMR titration. Moreover, PL reversibility of PtC + Ag⁺ could be achieved on addition of PMDTA.

Received 15th August 2014
Accepted 20th August 2014

DOI: 10.1039/c4ta04231j

www.rsc.org/MaterialsA

Introduction

The design of functional macromolecular structures and supramolecular metal complexes, by exploitation of self-assembly of complementary components via spontaneous and reversible supramolecular interactions, has the potential to create a myriad of fascinating molecular architectures.^{1–3} Supramolecular interactions have many advantages, such as (1) nanoscale ordering morphology can be controlled effectively by supramolecular interactions of active layers to move beyond the trial and error tuning of the device; (2) long-range order can be introduced to restore high charge-carrier mobilities for flexibility of devices, which offers the benefit of amorphous materials and is potentially cost effective in manufacture; (3) a direct method for assembling large numbers of molecules into structures via supramolecular organization can bridge length scales from nanometers to macroscopic dimensions for efficient long distance charge transport; (4) precise architectures can be controlled by the type and number of interactions (e.g. the photosynthetic reaction center in bacteria), where more

flexible systems are tolerant of physical deformations, such as cellular lipid bilayer membranes.^{4–6}

In the realm of modern supramolecular architectures, metal centered assemblies (MCs) governed by non-covalent interactions are promising candidates in designing functional electronic materials.^{7,8} Molecular organizations of these complexes regulated by a wide variety of non-covalent interactions are often ubiquitous in nature and play pivotal roles in many fields such as oxygen transport, gene activation, pharmaceuticals and catalysis.^{9,10} However, such functional supramolecular entities constituted with hydrogen-bonds and metal complexes are more specific and highly directional in both solutions and surfaces, and so are widely exploited in construction of three-dimensional supramolecular architectures in both chemical and biological systems.¹¹ However, both hydrogen-bonded and metal complexed entities have some advantages such as (1) convenient approaches towards precisely control of the geometries of electron donor-acceptor assemblies via hydrogen-bonded (H-bonded) interactions;^{12a,b} (2) 2.5-fold enhancement in photocurrent of photo-electrochemical devices incorporating components possessing complementary H-bonded units;^{12c,d} (3) enhancement of electron and hole transport as well as stability and even colors (pure colors to white light) potentially achieved in metal complexes as active layers;^{12e,f} (4) high thermal stabilities as well as greater charge transporting properties such as MLCT provided by metal complexes.^{12g,h}

Department of Materials Science and Engineering, National Chiao Tung University, Hsinchu 30049, Taiwan, ROC. E-mail: linhc@mail.nctu.edu.tw

† Electronic supplementary information (ESI) available: ¹H and ¹³C NMR, MALDI-TOF Spectra of PtC and characterizations of sensor complex. See DOI: 10.1039/c4ta04231j

Transition metal-based supramolecular MCs have recently emerged as a special area in supramolecular chemistry as they have crucial roles in catalysis, molecular-based electronic devices and well defined nanostructures at a molecular level.^{2b,13} Among these intriguing metals, platinum is in daily use owing to its anticancer chemotherapy applications.¹⁴ Despite the neurotoxicity of platinum drugs, a third-generation platinum drug oxaliplatin was approved for treatment of metastatic colorectal cancer by the US Food and Drug Administration (FDA).¹⁵ Apart from use in chemotherapy, platinum-based supramolecular MCs are reliable sources for next-generation molecular devices. Xing *et al.* reported an amphiphilic cationic platinum(II) terpyridyl ferrocene complex that formed a host-guest driven self-assembled vesicle structure.¹⁶ Shirakawa *et al.* demonstrated the formation of a one-dimensional structure using π - π and solvophobic interactions of an 8-quinolinol platinum(II) chelate derivative with a 3,4,5(*n*-dodecyloxy)-benzoylamide unit.¹⁷

Dendrimers have long been known as ideal flat-forms in designing multidimensional and multifunctional supramolecular hierarchical nano-architectures, because of their high branching points with easily achievable molecular symmetry at the nanoscale.¹⁸ The inherent directional excitation energy transfer (EET) capabilities of dendrimers have been used to prepare light-harvesting (LH) antennas in artificial photosynthesis. Dendritic nano-structured self-assemblies are prime constituents of novel nano-technological electronic devices.¹⁹ Moreover, new bottom-up synthetic approaches for dendritic MC nanostructures with control over sizes, surface properties, solubilities and compositions are highly desirable for formation of hierarchical MC-based self-assemblies. Shelnut *et al.* reported the first controlled photo-catalytic approach for synthesizing sheet-like nanodendrites or foam-like nano-sheets of platinum.²⁰ However, to the best of our knowledge a platinum complex core containing three peripheral uracil H-bonded units for creation of MC-based self-assemblies to engineer electron/energy transfer features has not yet been explored.

Metal-based organic complexes have long been used in molecule sensing applications because of their flexible energy transfer characteristics.²¹ However, despite their conventional applications in various fields, transition metals have posed a great threat to human health and environmental pollution over recent years. Silver ions can bind various metabolites, including carboxyl, amine, imidazole and sulfhydryl enzymes.²² Extreme bioaccumulation and ghastly toxic effects of silver ions make them intriguing targets to detect selectively.²³ Many small molecule-, polymer- and nanoparticle-based probes have been reported as silver ion detectors,²⁴ but often with low sensitivity. Thus, it is imperative to develop new metal complex-based probes for selective and sensitive detection of silver ions.

Herein, as shown in Fig. 1, we developed two H-bonded tetrads, PtC-(TPAD1)₃ and PtC-(TPAD2)₃, containing a central platinum complex (PtC) and two generations of terminal triarylamine dendrimers (TPAD1 and TPAD2 with electron-donating nature). We also studied the electron/energy transfers and self-assemblies of H-bonded tetrads by UV/Vis, PL, ¹H NMR

titrations, TRPL and AFM morphological studies. For the first time we evaluated the sensing ability of a metal complex core (PtC) with three uracil units in specific sensing of various metal ions, in which the PtC core selectively recognized Ag⁺ ions *via* binding with imidazole -NH unit, as verified by NMR-titrations. Importantly, the sensing mechanism of the metal complex core was completely reversible on addition of a tridentate ligand 1,1,4,7,7-pentamethyl-diethylenetriamine (PMDTA) solution.

Results and discussion

Molecular design

Fine tuning of counter H-bonded units with a central metal core and triple terminal dendritic units could be an ideal choice for realization of entrenched electron/energy transfers *via* branching units offered by tetrapod structures. Derivative 12 containing both terminal alkyne and uracil H-bonded units was synthesized from compound 1 using a modular multi-step synthetic approach as shown in Scheme 1. 2-(4-Bromo-2,5-bis(octyloxy-phenyl)-1*H*-1,3,7,8-tetraaza cyclopenta[1]phenanthrene platinum dichloride (derivative 16) was prepared starting from aldehyde 13 and phenanthroline diketone 14 using an acid catalyzed imidazole formation, which was coupled with PtCl₂(NH₂)₂ under reflux in DMSO solution (see Scheme 2).²⁵ A central platinum core (PtC) containing peripheral uracil H-bonded units was synthesized using compounds 12 and 16 *via* sonogashira coupling strategy as depicted in Scheme 3. The platinum complex core was completely characterized by ¹H and ¹³C NMR spectroscopies. Moreover, the abundant molecular ion peak in MALDI-TOF analysis (as shown in Fig. S1†) confirmed the formation of PtC. The exceptional nano-material properties of dendrimers and supramolecular self-assemblies and our previous success in designing novel supramolecular architectures prompted us to perform the aforementioned task.²⁶ Dendrimers TPAD1 and TPAD2 were prepared according to our previous synthetic protocols.²⁷ With two counter H-bonded building moieties in hand to further appreciate self-assembly properties, we fabricated supramolecular H-bonded tetrads PtC-(TPAD1)₃ and PtC-(TPAD2)₃ *via* a classical supramolecular non-covalent H-bonded approach by our previous report, as shown in Scheme 4.²⁷

IR spectral studies

To probe the multiple H-bonded interactions between the metal complex core (PtC) and dendritic H-bonded termini (TPAD1 and TPAD2), attenuated total reflection Fourier transform infrared (ATR-FTIR) measurements were carried out. As shown in Fig. 2, ATR-FTIR spectra of TPAD1, TPAD2 and PtC in CH₂Cl₂ showed free NH stretching bands at 3438, 3420 and 3176 cm⁻¹, respectively. The NH stretching bands of supramolecular tetrads PtC-(TPAD1)₃ and PtC-(TPAD2)₃ (1 : 3 stoichiometry) in CH₂Cl₂ were observed at 3327 and 3328 cm⁻¹, respectively, which confirmed the formation of multiple H-bonding between the complementary H-bonded core (PtC) and dendrimers (TPAD1 and TPAD2),²⁸ as noticed in Fig. 3.

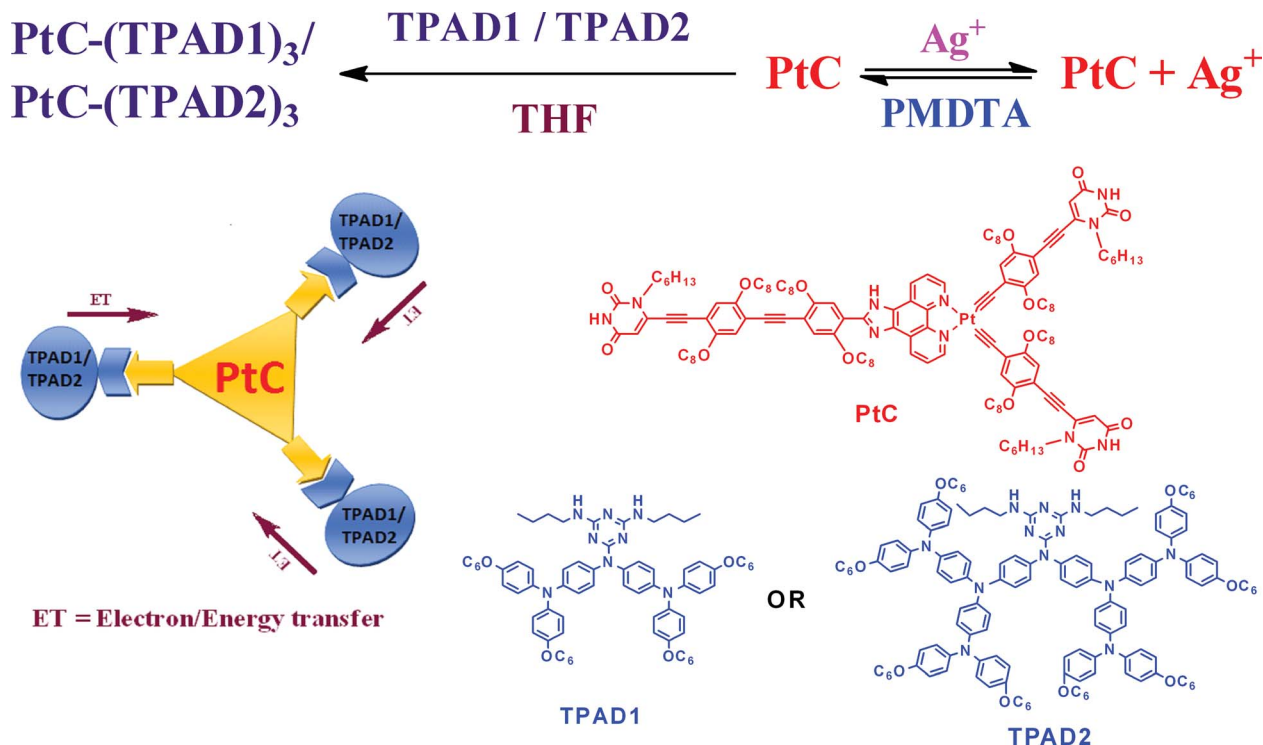


Fig. 1 Schematic representation of PtC sensor selectivity towards Ag⁺ and chemical structures of supramolecular tetrads PtC-(TPAD1)₃ and PtC-(TPAD2)₃ containing a platinum complex core (PtC) and two generations of three triarylamine dendrimers (TPAD1 and TPAD2).

¹H NMR titrations

To further corroborate the presence of multiple H-bonds in tetrads, we performed ¹H NMR titrations as shown in Fig. 4, in which PtC concentration was kept constant at 10 mM and the concentrations of dendrimers TPAD1 and TPAD2 were increased up to 3.5 equivalents with an equal span of 0.5 equivalent. While increasing the dendrimer concentrations in the range of 0–3.5 equivalents, the NH protons of PtC showed upfield shifts in both supramolecular tetrads from 11.08 to 9.71 ppm and from 11.08 to 9.65 ppm for PtC-(TPAD1)₃ and PtC-(TPAD2)₃, respectively. As noticed in Fig. 4, downfield shifts of PtC-NH protons were also well evidenced for the formation of multiple H-bonds in the supramolecular complexes as per the literature.²⁹ To further assess the multiple H-bonded interactions and the electron/energy transfer features between counter H-bonded moieties, we performed UV-Vis and PL titrations in chloroform solvent medium.

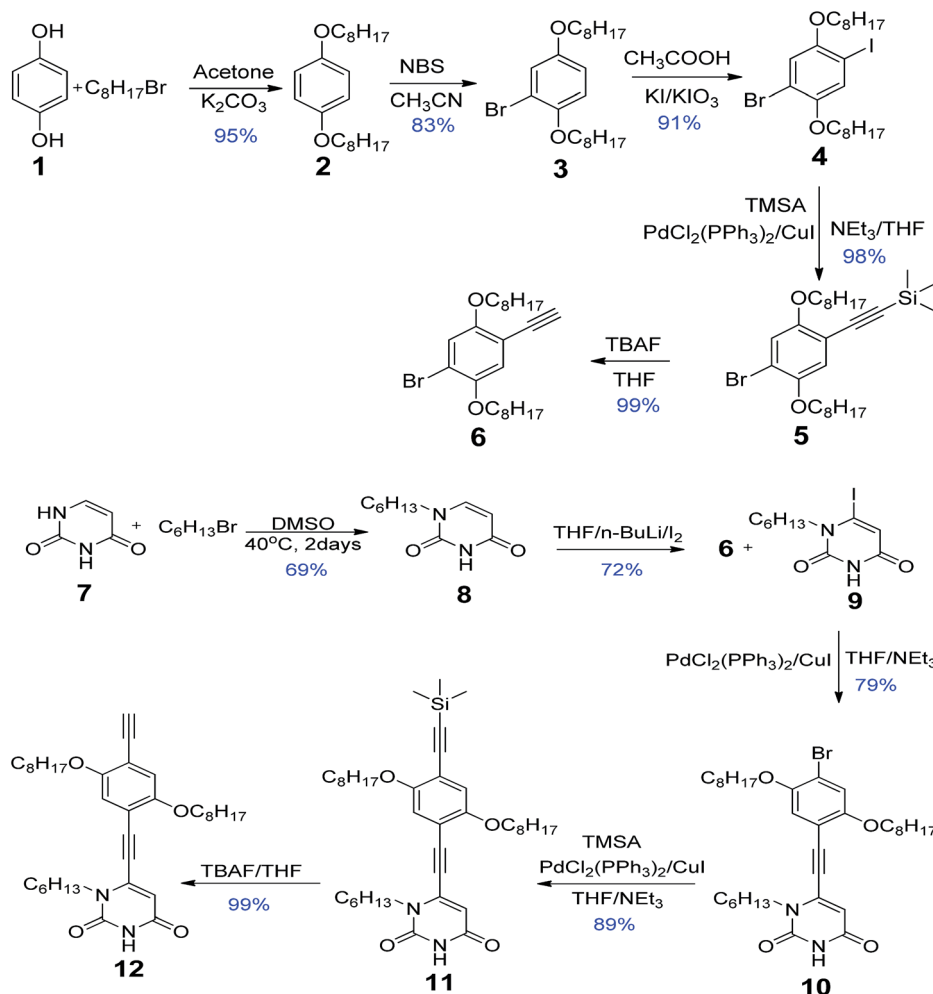
UV-Vis and PL titrations

UV-Vis and PL titration experiments in chloroform were performed to study the interactions of both dendrimers (TPAD1 and TPAD2) with the metal complex core PtC. Upon adding aliquots of TPAD1 to PtC, a bathochromic shift (Fig. 5a) from 408 to 413 nm was observed for the platinum complex absorption maximum corresponding to the S₀-S₁ electronic transition of PtC-(TPAD1)₃. A similar red-shift in PtC-(TPAD2)₃, *i.e.* from 408 to 415 nm (Fig. 5b), was observed during the UV-Vis titrations. During UV-Vis titrations, dendrimers TPAD1 and TPAD2

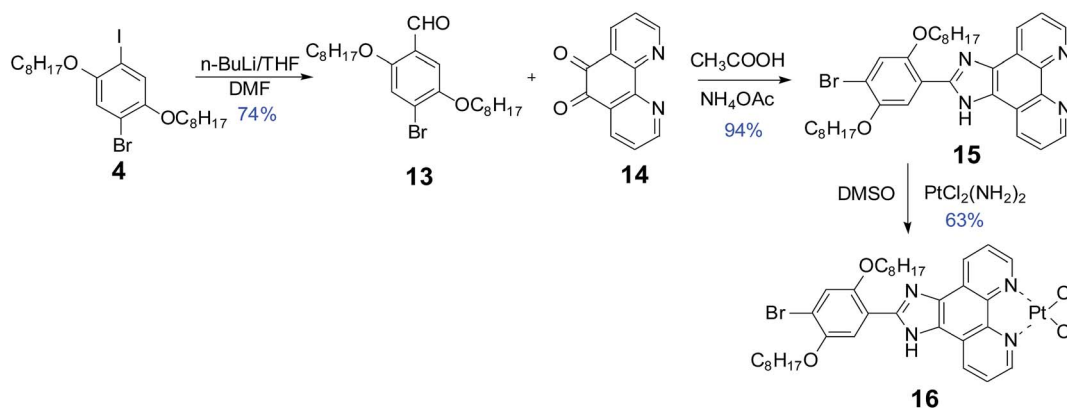
showed isosbestic points at 372 and 393 nm, respectively, which arose from the formation of multiple H-bonded tetrads in chloroform solution. Simultaneously, the PL titrations of both supramolecular tetrads (Fig. 5c and d) showed bathochromic shifts in PtC-(TPAD1)₃ (from 461 nm to 466 nm) and PtC-(TPAD2)₃ (from 461 nm to 468 nm). Both results of UV-Vis and PL titrations verified the metal complex core aggregations of PtC in both supramolecular tetrads. Similar to conventional J-aggregated dyes,³⁰ our supramolecular tetrads showed enhanced PL titrations during the formation of H-bonded structures, where the PL emission intensities of PtC were enhanced (λ_{ex} = 405 nm) by adding both dendrimers (TPAD1 and TPAD2 with electron-donating units). This consequence was rationalized by an electron/energy-transfer process from the dendrimers TPAD1 and TPAD2 to the platinum complex core PtC. The observed UV-Vis and PL titration trends further confirmed a molar ratio of 1 : 3 as PtC H-bonded to both TPAD1 and TPAD2 to form supramolecular tetrads PtC-(TPAD1)₃ and PtC-(TPAD2)₃, respectively.

TRPL spectra of energy transfers in H-bonded tetrads

To further evaluate the characteristics of energy transfers between H-bonded tetrads, we conducted TRPL measurements for both tetrads PtC-(TPAD1)₃ and PtC-(TPAD2)₃. Previous studies of metal-centered complexes revealed that energy transfers arose from branched ends to metal centers.³¹ Ventura *et al.* reported the energy transfer dynamics in multi-chromophoric arrays engineered from phosphorescent Pt(II)/Ru(II)/Os(II) centers linked to a central truxene platform.³² They



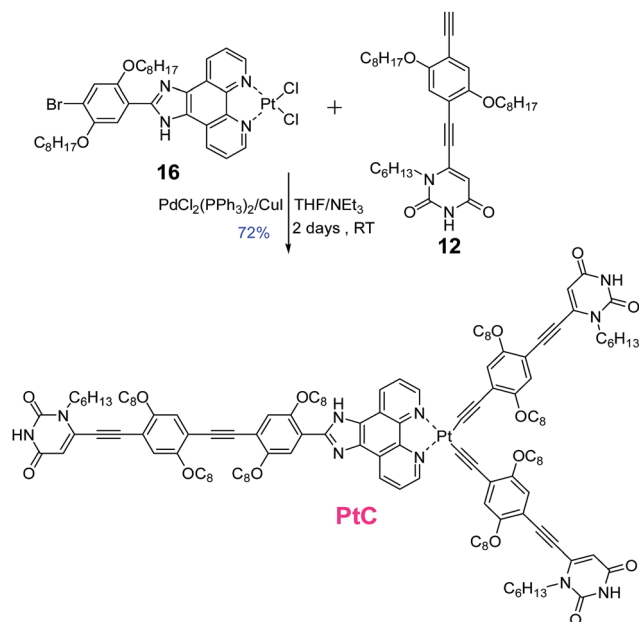
Scheme 1 Synthetic procedure of compound 12.



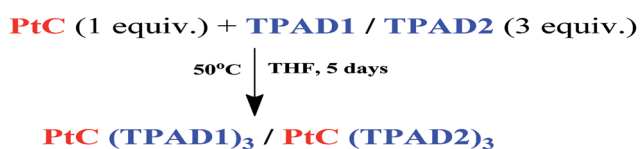
Scheme 2 Synthetic procedure of compound 16.

reported that the electronic properties of the Ru and Os subunits in the arrays were unaffected by the presence of the truxene core, whereas direct linking of the Pt subunit to the truxene *via* the σ -alkyne bond markedly influenced the spectroscopic behavior of the Pt center as evidenced by the TRPL studies (lifetime of 4.3 s for the mono ethynyl-bipy substituted

truxene and 17.5 ms for the bis ethynyl-bipy substituted truxene). Therefore, the direct linking of uracil units in PtC through alkyne linkage would enhance energy transfers as evidenced by TRPL spectral studies. Similar to metal organic frameworks, multiple H-bonded assemblies demonstrated energy transfers as illustrated in previous reports.³³ Zhang *et al.*



Scheme 3 Synthetic procedure of PtC.

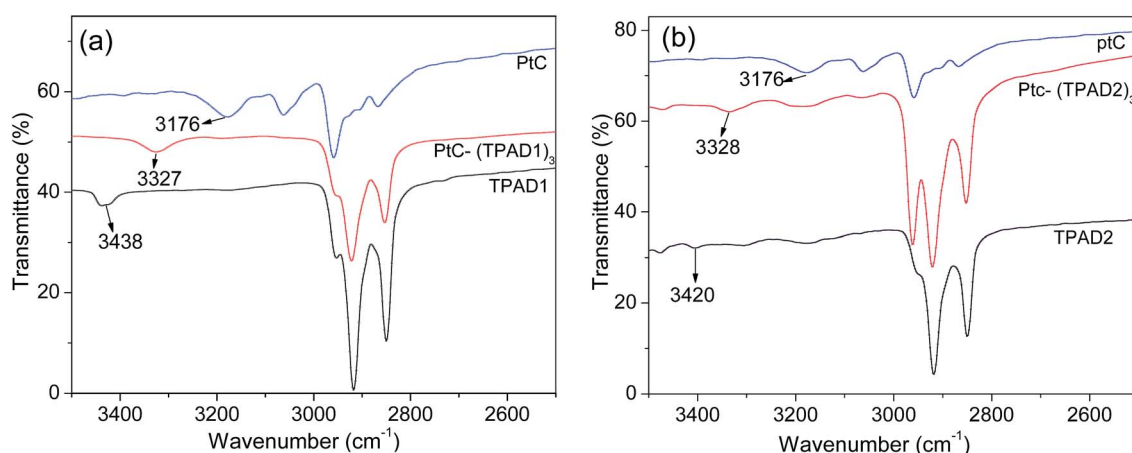
Scheme 4 Synthesis of H-bonded tetrads PtC-(TPAD1)₃ and PtC-(TPAD2)₃.

established the photoinduced electron transfer and charge-recombination in 2-ureido-4[1*H*]-pyrimidinone quadruple H-bonded porphyrin–fullerene assemblies, which were also well recognized through time-resolved studies.³⁴ In addition, steady-state and time-resolved spectroscopies demonstrated that upon excitation of the porphyrin, electron transfers to the fullerene occurred with rate constants of $1.6 \times 10^8 \text{ s}^{-1}$ (60%) and $4.2 \times 10^8 \text{ s}^{-1}$ (44%) for assemblies **I** and **II**, respectively, in a

CH_2Cl_2 solution at room temperature. Therefore, the combination of both organic metal framework and H-bonded assemblies would provide greater energy transfers as reported previously.³⁵ Hence we carried out TRPL studies as illustrated in Fig. 6a and b. The energy transfers occurred during tetrad formations of metal complex core **PtC** with various molar ratios of dendrimers (**TPAD1** and **TPAD2**) through TRPL spectral changes. As summarized in Table S1,[†] we found that the fluorescence decay constants (τ) were affected typically by the energy transfers in both tetrads [**PtC**-(**TPAD1**)₃ and **PtC**-(**TPAD2**)₃]. The average decay constants (τ_{avg}) of **PtC** were enhanced from 3.70 to 6.43 and 8.11 ns for **PtC**-(**TPAD1**)₃ and **PtC**-(**TPAD2**)₃, respectively. The longer decay time values of H-bonded tetrads were attributed to the energy transfer contribution from complementary dendrimers, which appeared in the results of bi-exponential decay fittings. Similar to the changes of average decay constants (τ_{avg}), the faster decay component (A_1) of **PtC** (28.3%) was increased to 45.2% and 47.1%, respectively, for both tetrads [**PtC**-(**TPAD1**)₃ and **PtC**-(**TPAD2**)₃]. On the other hand, the longer decay component (A_2) of **PtC** (71.7%) was reduced to 54.8% and 52.9%, respectively, for both tetrads [**PtC**-(**TPAD1**)₃ and **PtC**-(**TPAD2**)₃], which also occurred in chelation of Cu^{2+} and Ni^{2+} ions to our previous sensor polymers.³⁶ As a result of *J*-aggregated assembly of both tetrads [**PtC**-(**TPAD1**)₃ and **PtC**-(**TPAD2**)₃], rapid changes in the lifetime of **PtC** were evidenced from the experimental data, which confirmed electron/energy transfers from triarylamine dendrimers (**TPAD1** and **TPAD2**) to the platinum complex core (**PtC**) as shown in Fig. 1 and 3. These results show that H-bonded assemblies consisting of different kinds of building blocks, including a platinum complex core (**PtC**) and two generations of triarylamine dendrimers (**TPAD1** and **TPAD2**), are attractive for construction of supramolecular metallo-dendrimers by the self-assembly technique.

AFM studies

Encouraged by the studies described above in deducing the energy transfer features between counter H-bonded components, we were further intrigued to investigate the

Fig. 2 ATR-FTIR spectra of H-bonded tetrads PtC-(TPAD1)₃ and PtC-(TPAD2)₃ in CH_2Cl_2 with 3 : 1 molar ratio of (a) TPAD1 and PtC (b) TPAD2 and PtC.

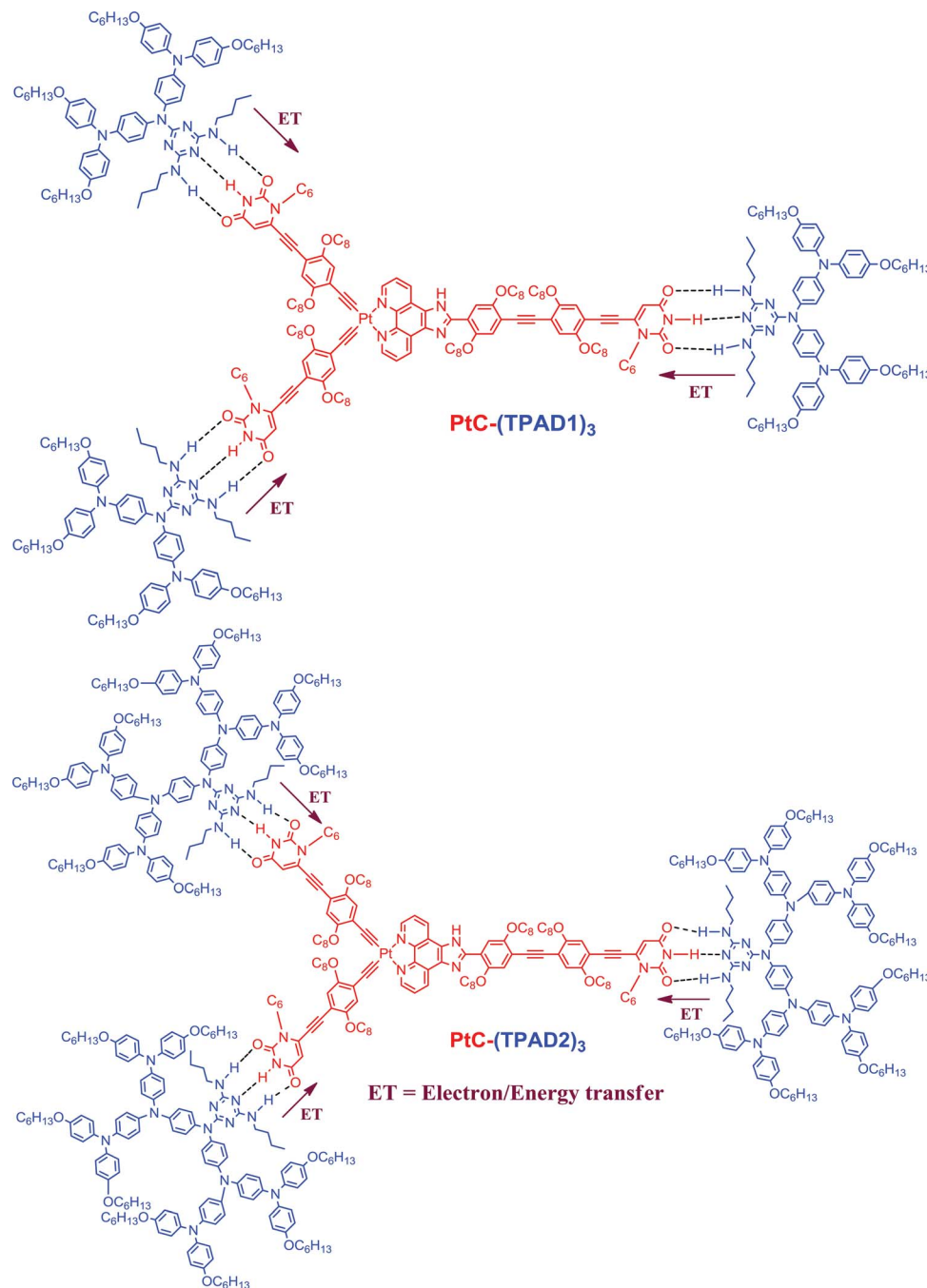


Fig. 3 Chemical structures of supramolecular tetrads $\text{PtC}-(\text{TPAD1})_3$ and $\text{PtC}-(\text{TPAD2})_3$ containing a platinum complex core (PtC) and two generations of H-bonded triarylamine dendrimers TPAD1 and TPAD2, respectively.

morphological changes of these tetrads to understand self-assembly phenomena at the nanoscale. Multiple H-bonded arrays have been shown to be versatile tools for preparation of functional supramolecular materials in solution. We report the results obtained by designing and engineering a novel library of shape persistent molecular modules able to transfer their geometrical information to the final supramolecular tetrad architectures through formation of $\text{PtC}-(\text{TPAD1})_3$ and $\text{PtC}-(\text{TPAD2})_3$ complexes at the nanoscopic level. Previously, Sun *et al.* reported the morphology and chirality of supercoils demonstrating photoresponsiveness through AFM studies,

which were induced from photoisomerization of the azobenzene components within the self-assembled nanostructures.^{37a} Similarly, the utility of an external structure-directing agent to induce orthogonal H-bonding-mediated programmed supramolecular-assembly *via* AFM analysis and gelation of an n-type NDI chromophore was reported by Ghosh *et al.*^{37b} Additionally, there are many reports that the presence of multiple H-bonds has provided self-assemblies with nano-level aggregations.³⁷ As shown in Fig. 7, atomic force microscopy (AFM) images of metal complex core PtC and both generations of tetrads were measured and investigated. Upon H-bonding

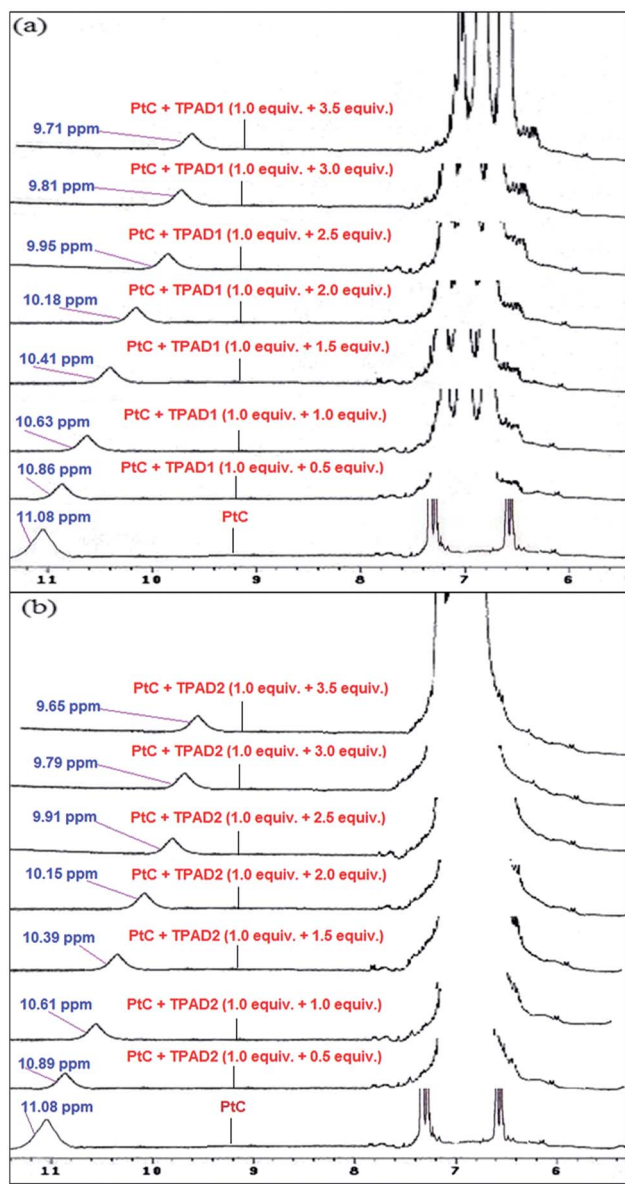


Fig. 4 ^1H NMR titrations of PtC with (a) TPAD1 and (b) TPAD2 (PtC was fixed at 1 equivalent and the concentrations of TPAD1 and TPAD2 were increased up to 3.5 equivalents with an equal span of 0.5 equivalent in d-chloroform).

with metal complex core PtC, the roughnesses of tetrads PtC-(TPAD1)₃ and PtC-(TPAD2)₃ were reduced to different extents because of their self-assemblies, where the roughnesses of PtC, PtC-(TPAD1)₃ and PtC-(TPAD2)₃ were around 123 nm, 17 nm and 5.1 nm, respectively. Hence, this also confirmed that self-assemblies provided different degrees of uniform aggregations in two generations of tetrads to enhance the electron/energy transfers.

Sensor properties of PtC

Because of its excellent photophysical properties, PtC (0.1 μM) in THF was initially investigated towards 1000 μM of metal ions (Li^+ , Ag^+ , K^+ , Na^+ , Cs^+ , Ni^{2+} , Fe^{3+} , Co^{2+} , Zn^{2+} , Cd^{2+} , Pb^{2+} , Ca^{2+} ,

Cr^{3+} , Mg^{2+} , Cu^{2+} , Mn^{2+} , Hg^{2+} , Fe^{2+} and Ag^{2+}) in H_2O . As shown in Fig. 8 and 9, PtC showed better selectivity towards Ag^+ , whereas other metal ions had negligible sensitivities to PtC. Sensor selectivity of PtC towards Ag^+ was further confirmed by single and dual metal analysis as follows: during single metal analysis of PtC (Fig. 8), Ag^+ provided a huge fluorescence quenching in PtC + Ag^+ , where the PL intensity ($I = 261$ at 461 nm for PtC + Ag^+) was 36-fold reduced in contrast with PtC ($I_0 = 9694$ at 461 nm), and all other metal ions exhibited trivial responses. Similarly, the greater selectivity of PtC towards Ag^+ (1000 μM) in the presence of other metal ions (1000 μM) was evidenced in the background metal analysis of PtC (Fig. S2[†]). In both cases, sensor selectivity of PtC towards Ag^+ was further confirmed by Stern-Volmer quenching constant values, as summarized in Table S2.[†] Stern-Volmer quenching constant (K_{SV}) of PtC + Ag^+ was found to be $3.61 \times 10^4 \text{ mol}^{-1}$, and other metal ions were in the range of 10^2 mol^{-1} .

Sensor titration of PtC with Ag^+

Upon titration of PtC (0.1 μM) with Ag^+ (0–1000 μM with an equal span of 100 μM in H_2O), the PL intensity of PtC at 461 nm was quenched slowly (Fig. 10). Similarly, PL quenching of PtC was well established in Fig. S3[†] and the detection limit of Ag^+ by PtC was calculated as $5.54 \times 10^5 \text{ M}$ by standard deviation and linear fittings, as shown in Fig. S4.[†] The linear fluorescent quenching of PtC upon addition of Ag^+ ions may arise from binding of Ag^+ with the imidazole unit of PtC. However to confirm the above assumption, we extended our investigation by NMR titration of PtC with Ag^+ to establish the binding site as detailed below.

Stoichiometry and binding site of PtC + Ag^+

In general, stoichiometry tests of sensor complexes can give a clear idea of their binding sites. However, because of the low concentration of PtC (0.1 μM) in the sensor titration with higher concentrations of Ag^+ (0–1000 μM with an equal span of 100 μM), the stoichiometry of PtC + Ag^+ was not calculated from UV/PL titrations. Hence, to calculate the stoichiometry and binding site of PtC + Ag^+ , the ^1H NMR titration was carried out as shown in Fig. 11. The ^1H NMR titration of PtC in d_8 -THF (10 mmol) with Ag^+ in D_2O (0–10 mmol with an equal span of 2 mmol) established the stoichiometry and binding site towards the sensor response. Interestingly, the -NH peak of the imidazole group in PtC diminished slowly with increasing concentration of Ag^+ in D_2O . However, the remaining ^1H NMR peaks were not affected (Fig. 11). Moreover, the ^1H NMR titration of PtC with Ag^+ confirmed the 1 : 1 stoichiometry of PtC + Ag^+ as well. As the -NH imidazole peak of PtC was not affected after 0.8 equiv. addition of Ag^+ in D_2O , the 1 : 1 stoichiometry of PtC + Ag^+ was further proven. Similarly, the binding site of PtC + Ag^+ was further verified by the reversibility test of PtC + Ag^+ through the addition of few drops of PMDTA in THF.³⁸ As shown in Fig. S5,[†] fluorescence emission of PtC was restored on the addition of PMDTA, hence the dissociation of complex PtC + Ag^+ was proven. The photograph of sensor reversibility of PtC + Ag^+ on addition of PMDTA also supports this idea (Fig. 12).

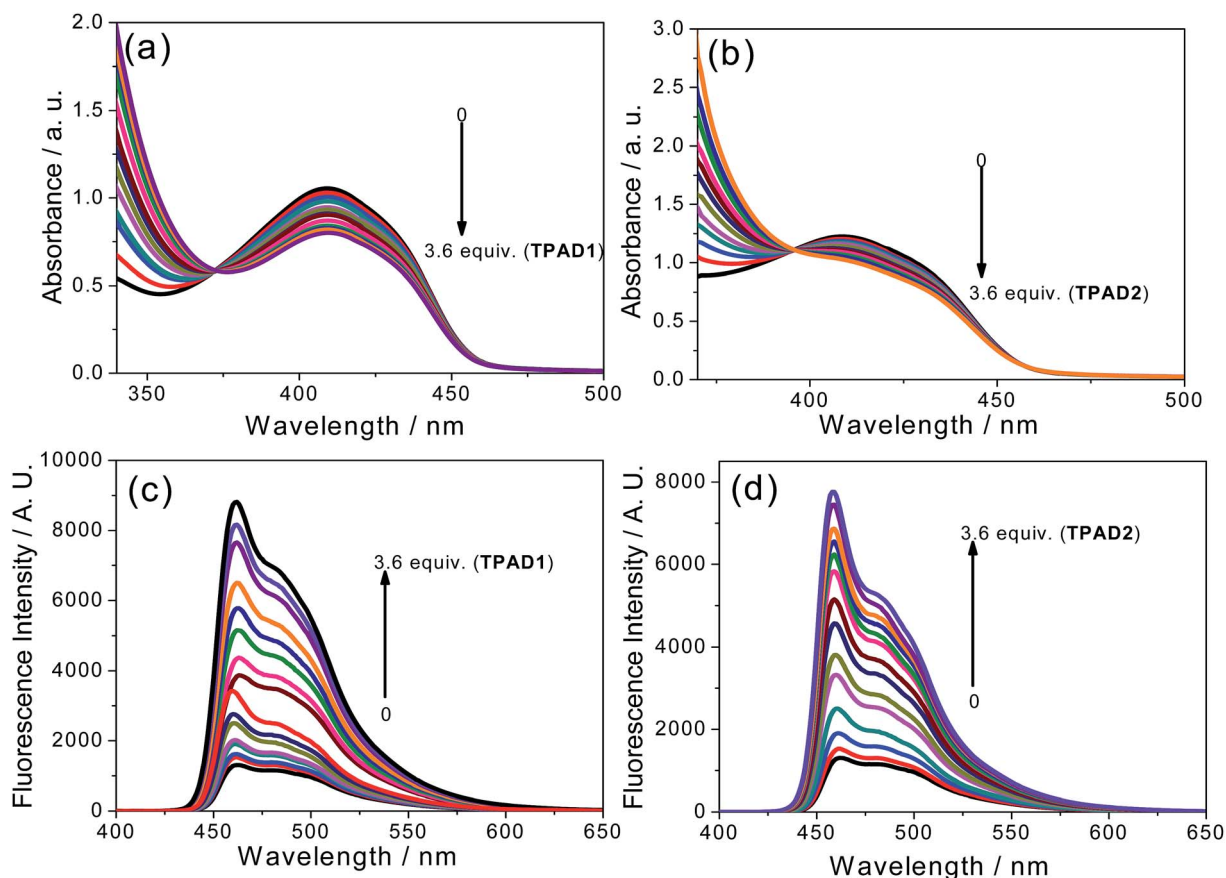


Fig. 5 UV-Vis and PL spectra of PtC upon titrations of (a and c) TPAD1 and (b and d) TPAD2 (PtC was fixed at 1 equivalent and the concentrations of TPAD1 and TPAD2 were increased up to 3.6 equivalents with an equal span of 0.3 equivalent in chloroform).

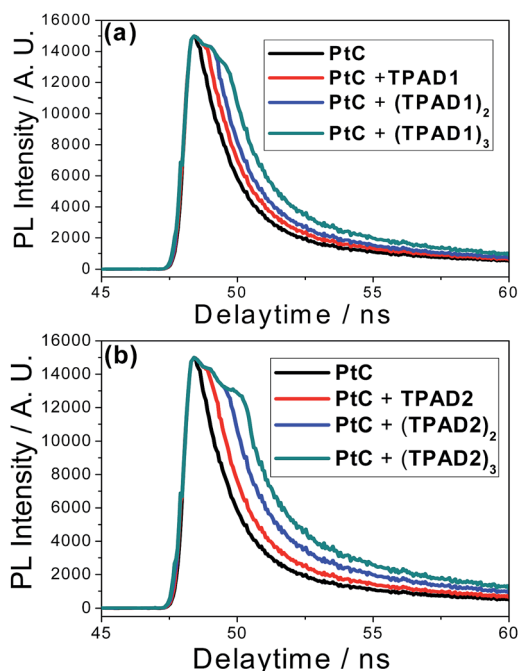


Fig. 6 (a) and (b) TRPL spectra of PtC with increasing concentrations of TPAD1 and TPAD2, respectively. (0–3.0 equiv. with an equal span of 1 equiv.).

Therefore, a possible binding mechanism of PtC towards Ag^+ was proposed as shown in Fig. S6.† However, to further confirm the imidazole binding site, we attempted to carry out sensor titrations with compounds 15 and 16. However, because of multiple binding sites in 15 (two phenanthroline nitrogens) and low solubility of 16 in THF, we were unable to obtain their sensor properties from both compounds. As reported in the literature and from our previous results³⁹ (Fig. S7†), we found that the fluorescence decay constants (τ) were affected typically by turn-off sensor responses, as summarized in Table S1.† From the TRPL signals without any sensor responses, the fluorescence lifetime values of PtC were reduced from 3.70 ns to 2.95 ns. During the sensing process of PtC + Ag^+ , a faster decay component (A_1) of PtC (28.3%) was increased to 76.2%, along with 71.7% of a longer decay component (A_2) reduced to 23.8%, as shown in Table S1.†

Conclusions

In this study, we designed and synthesized a novel metal complex PtC possessing a central platinum core and three terminal uracil H-bonded units *via* a modular synthetic approach. For the first time, a PtC complex was successfully synthesized for use as a selective sensor probe towards Ag^+ recognition and to be self-assembled with two complimentary

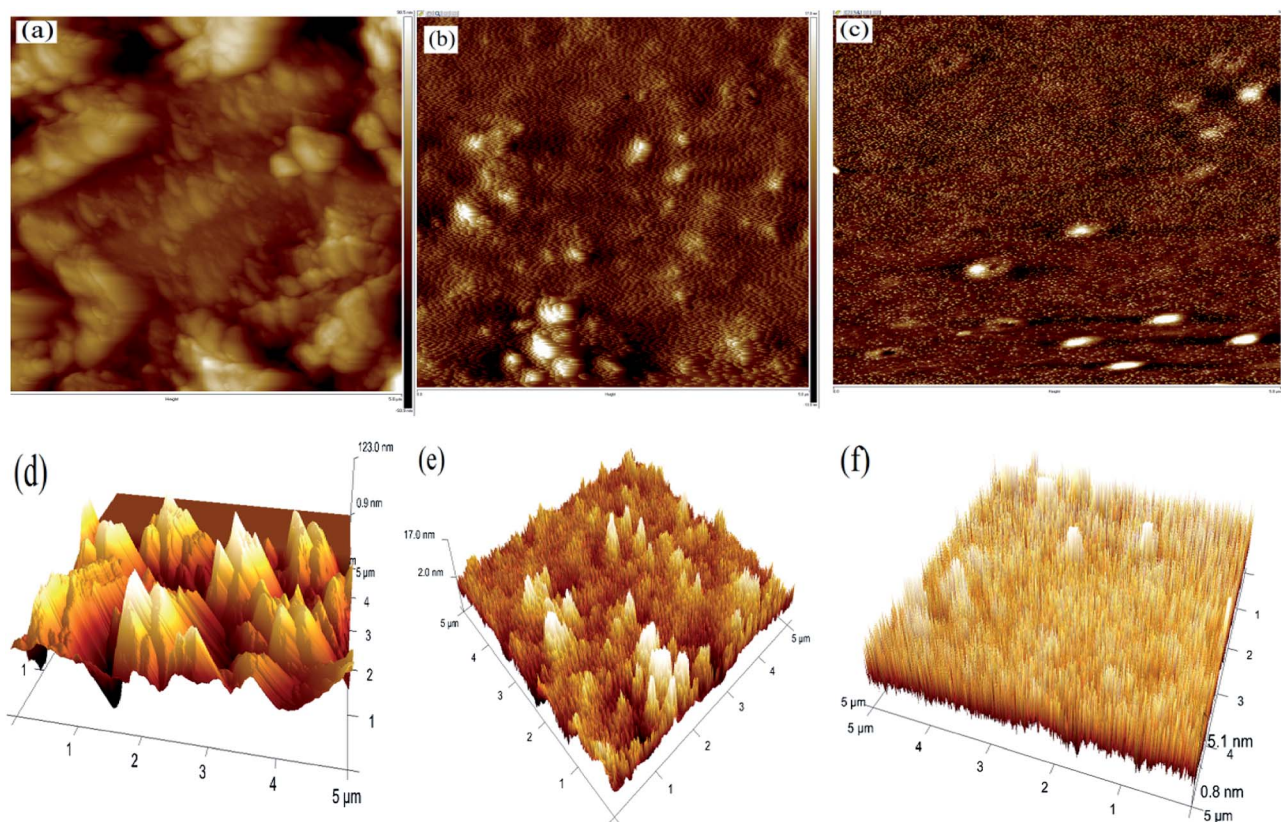


Fig. 7 AFM height and 3D images of (a and d) PtC, (b and e) PtC-(TPAD1)₃, (c and f) PtC-(TPAD2)₃. Scale bar 5 μm.

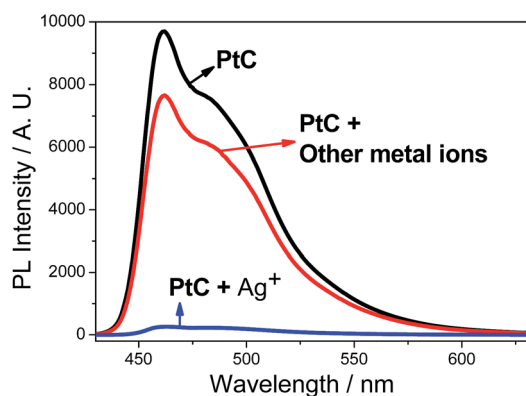


Fig. 8 Sensor selectivity of PtC (*i.e.* responses of PL intensities at 461 nm) towards various metal ions; where PtC concentration is 0.1 μM and the metal ion concentration is 1000 μM ($\lambda_{\text{ex}} = 405 \text{ nm}$ & $\lambda_{\text{em}} = 461 \text{ nm}$).

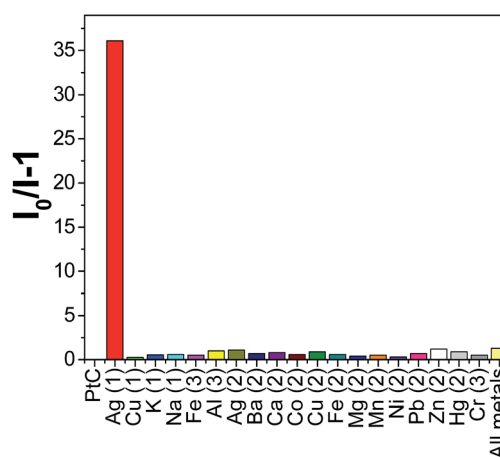


Fig. 9 PtC sensor selectivity towards metal ions (I_0 : initial PL intensity of PtC; I : PL intensity of PtC with metal ions); where PtC concentration is 0.1 μM and the metal ion concentration is 1000 μM.

dendrimers, TPAD1 and TPAD2, to form novel H-bonded tetrads PtC-(TPAD1)₃ and PtC-(TPAD2)₃, respectively. The existence and preservation of multiple H-bonds in both tetrads were demonstrated by ¹H NMR titration, as well as IR and TRPL spectral studies. Furthermore, electron/energy transfer features in these tetrads were established by UV-Vis and PL titrations of PtC with two generations of dendrimers, TPAD1 and TPAD2, with electron-donating units. Self-assembled nanostructural formation with smoother surface roughness in tetrads compared with its precursors in AFM studies further affirmed

self-assembly at the nanoscale. Exclusively, the PtC core showed a better selective and sensitive metal recognition capability towards Ag⁺ without interference from commonly encountered transition metals. The 1 : 1 stoichiometry of Ag⁺ complex formed during the sensing event was established by ¹H NMR titration profiles. Remarkably, on-off-on reversible etiquette formation by Ag⁺ and PMDTA was successfully achieved. Thus, we believe that the findings in this study illuminate the field of

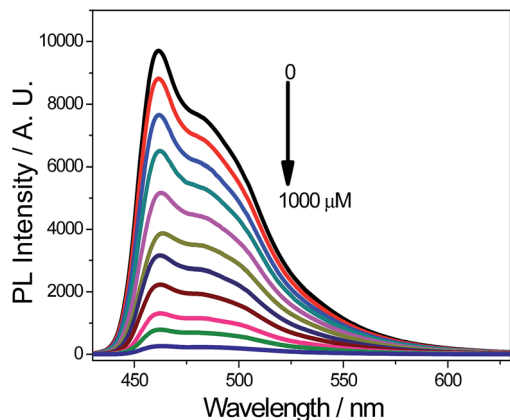


Fig. 10 PL titration of PtC (0.1 μM) with Ag^+ (0–1000 μM) by increasing concentration with an equal span of 100 μM .

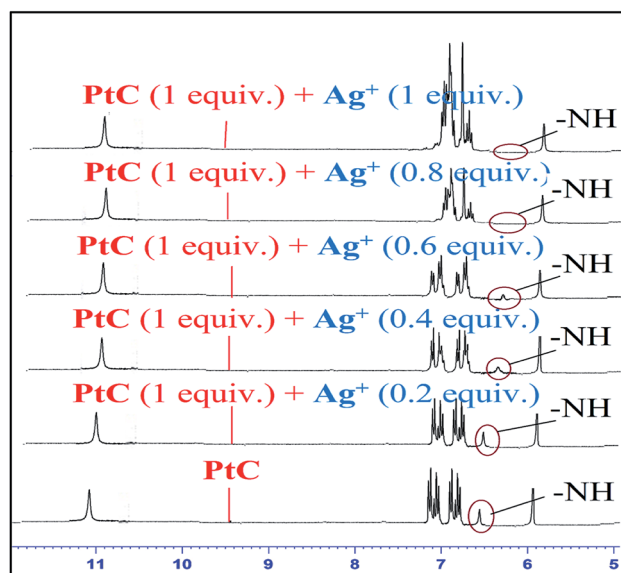


Fig. 11 ^1H NMR titration of PtC (10 mmol in $\text{d}_8\text{-THF}$) with Ag^+ by increasing concentration (0–10 mmol) with an equal span of 2 mmol in D_2O .

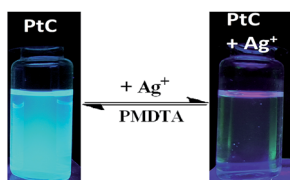


Fig. 12 Photographs of titrations of PtC with reversible (on-off-on) fluorescence changes towards Ag^+ and its reversibility on further addition of PMDTA (under UV lamp with $\lambda_{\text{ex}} = 365 \text{ nm}$ & $\lambda_{\text{em}} = 461 \text{ nm}$).

metal complexed nano-self-assembled structures. Furthermore, opto-electronic applications of these H-bonded tetrads are currently under way in our laboratory.

Experimental

Materials and methods

All anhydrous reactions were carried out by standard procedures under nitrogen atmosphere to avoid moisture, and all solvents were dried by distillation over appropriate drying agents. Reactions were monitored by TLC plates and column chromatography was generally performed on silica gel. ^1H and ^{13}C NMR spectra were recorded on a 300 MHz spectrometer. The chemical shifts (δ) in ppm and coupling constants (J) in Hz were obtained relative to TMS (0.00) and d-chloroform (7.26 & 77.0) for ^1H and ^{13}C NMR spectra (s, d, t, q, m and br mean single, double, ternary, quadruple, multiple and broad single, respectively). Mass spectra (MALDI and FAB) were acquired on the respective mass spectrometers. Elemental analysis was carried out by Elemental Vario EL. ATR-FTIR spectra were measured using a Perkin Elmer spectrum 100 series spectrometer, and were collected at a resolution of 4 cm^{-1} using a deuterated triglycine sulfate detector by averaging four scans. Absorption and fluorescence spectra were measured on the V-670 Spectrophotometer and F-4500 Fluorescence Spectrophotometer, respectively. Identification and purity of the intermediates were characterized by NMR (^1H & ^{13}C), mass (MALDI and FAB) and melting point measurements. The synthesis of final dendrimers TPAD1 and TPAD2 was as reported previously.²⁷ Compounds TPAD1, TPAD2 and PtC were dissolved in CHCl_3 at $1 \times 10^{-5} \text{ M}$, for UV/Vis and PL titrations. Both tetrads PtC-(TPAD1)₃ and PtC-(TPAD2)₃, obtained from Scheme 4, were dissolved in CHCl_3 and their solid films were prepared by spin coating and then measured. Time-resolved photoluminescence (TRPL) spectra were measured using a home-built single photon counting system. Excitation was performed using a 450 nm diode laser (Picoquant PDL-200, 50 ps fwhm, 2 MHz). The signals collected at the excitonic emissions of solutions were connected to a time-correlated single photon counting card (TCSPC, Picoquant Timeharp 200). Emission decay data were analyzed with biexponential kinetics in which two decay components were derived. Lifetime values (τ_1 and τ_2) and pre-exponential factors (A_1 and A_2) were determined and summarized. Li^+ , Ag^+ , K^+ , Na^+ , Cs^+ , Ni^{2+} , Fe^{3+} , Co^{2+} , Zn^{2+} , Cd^{2+} , Pb^{2+} , Ca^{2+} , Cr^{3+} , Mg^{2+} , Cu^{2+} , Mn^{2+} , Hg^{2+} , Fe^{2+} and Ag^{2+} metal ions were dissolved in water medium at $1 \times 10^{-3} \text{ M}$ concentration from their respective chloro compounds and PtC was dissolved in THF medium at $1 \times 10^{-7} \text{ M}$ concentration.

Synthesis of 1,4-bis-octyloxy-benzene (2). To a 500 mL flask containing 10 g (9 mmol) of hydroquinone (1) in 200 mL of DMF, 37 mL (22.5 mmol; 2.5 equiv.) of 1-bromohexane was added and refluxed for 36 h under N_2 atmosphere. Then, the mixture was cooled to room temperature and water was added. The precipitate was filtered and dried *in vacuo* for 3 h, then recrystallized with ethanol to afford the pure compound. Yield: 28.86 g (95%); ^1H NMR (300 MHz, CDCl_3): 6.82 (s, 4H), 3.90 (t, $J = 6.0 \text{ Hz}$, 4H), 1.74–1.65 (m, 4H), 1.34–1.27 (m, 20H), 0.88 (t, $J = 6.6 \text{ Hz}$, 6H).

Synthesis of 2-bromo-1,4-bis-octyloxy-benzene (3). 10 g (29.9 mmol) of compound 2 was dissolved in 100 mL of CH_3CN in a

250 mL flask under N₂ atmosphere. 5.5 g (32.9 mmol; 1.1 equiv.) of *N*-bromosuccinimide (NBS) was added portionwise and stirred for 24 h. Excess solvent was distilled out. The crude product was purified by column (SiO₂) by 99 : 1 hexane–EtOAc to afford a colorless oil. Yield: 10.26 g (83%); ¹H NMR (300 MHz, CDCl₃): 7.12 (s, 1H), 6.80 (s, 2H), 3.95 (t, *J* = 6.0 Hz, 2H), 3.88 (t, *J* = 6.0 Hz, 2H), 1.83–1.72 (m, 4H), 1.30–1.49 (m, 20H), 0.88 (t, *J* = 6.6 Hz, 6H).

Synthesis of 1-bromo-4-iodo-2,5-bis-octyloxy-benzene (4). 5 g (12.1 mol) of compound 3 was dissolved in a CH₃COOH–H₂O–conc. H₂SO₄ (95 : 3 : 2) mixture and heated to 80 °C for 30 minutes, then cooled to 50 °C and 1.3 g (0.78 mmol) of KI and 0.91 g (0.43 mmol) of KIO₃ was added and refluxed at 80 °C for 24 h. After cooling to room temperature, the mixture was quenched with Na₂SO₄ and then extracted with hexane. The pure compound 4 was obtained by column chromatography (SiO₂) 99 : 1 hexane–EtOAc to afford a white solid. Yield: 5.94 g (91%); ¹H NMR (300 MHz, CDCl₃): 7.26 (s, 1H), 6.96 (s, 1H), 3.92 (t, *J* = 6.0 Hz, 4H), 1.82–1.76 (m, 4H), 1.34–1.48 (m, 20H), 0.89 (t, *J* = 6.0 Hz, 6H).

Synthesis of 4-bromo-2,5-bis-octyloxy-phenylethynyl-trimethyl-silane (5). To 5 g (9.3 mmol) of compound 4 in a 250 mL flask purged with continuous N₂ atmosphere, 39 mg (0.05 mmol) of PdCl₂(PPh₃)₂ and CuI (0.05 mmol) were added with constant stirring. Then, 5 mL of freshly distilled THF was added *via* syringe and stirred for 10 minutes. Thereafter, Et₃N 45 mL was added and then heated to 50 °C. 1.32 mL (9.3 mmol; 1 equiv.) of TMSA was added and refluxed at 50 °C for 12 h and monitored *via* TLC. After completion, the mixture was cooled to RT, and the excess solvent was quenched and distilled out. The product was purified through column (SiO₂) 9 : 1 hexane–EtOAc to afford a yellow solid. Yield: 4.63 g (98%); ¹H NMR (300 MHz, CDCl₃): 7.08 (s, 1H), 6.94 (s, 1H), 3.94 (t, *J* = 6.0 Hz, 4H), 1.81–1.74 (m, 4H), 1.49–1.29 (m, 20H), 0.89 (t, *J* = 6.0 Hz, 6H), 0.25 (s, 9H).

Synthesis of 1-bromo-4-ethynyl-2,5-bis-octyloxy-benzene (6). 4.5 g of compound 5 was dissolved in THF with two drops of water with constant stirring, and then a few drops of tetrabutyl ammonium fluoride (TBAF) were added and stirred for 3 h. Monitored by TLC, upon completion of the reaction, the solvent was distilled out and purified through column (SiO₂) 9 : 1 hexane–EtOAc to afford a yellow solid, which was processed for the next step immediately. Yield: 3.83 g (99%); ¹H NMR (300 MHz, CDCl₃): 7.07 (s, 1H), 6.96 (s, 1H), 3.96 (t, *J* = 6.0 Hz, 4H), 3.28 (s, 1H), 1.84–1.74 (m, 4H), 1.46–1.28 (m, 20H), 0.88 (t, *J* = 6.0 Hz, 6H).

Synthesis of 1-hexyluracil (8). K₂CO₃ (14.80 g, 107.05 mmol) was added to a suspension of uracil (10.0 g, 89.21 mmol) in DMSO (150 mL) and stirred for 15–20 min at 45 °C. 1-Bromohexane (3.5 mL, 25 mmol) was added and the reaction mixture was stirred for 48 h. The reaction was cooled to room temperature and poured into cold water. The product was extracted three times with DCM, and washed with dilute HCl, water, brine, and dried over Mg₂SO₄. The organic layer was concentrated and poured into cold hexane with vigorous stirring. The resulting precipitate was filtered and washed with cold hexane to afford compound 8 (17.88 g, 69%) as a white solid. ¹H NMR

(300 MHz, CDCl₃): 9.12 (br, 1H), 7.14 (d, *J* = 9.0 Hz, 1H), 5.70 (d, *J* = 6.0 Hz, 1H), 3.71 (t, *J* = 7.5 Hz, 2H), 1.68–1.64 (m, 2H), 1.30–1.28 (m, 6H), 0.87 (t, *J* = 6.6 Hz, 3H).

Synthesis of 1-hexyl-6-iodouracil (9). At 78 °C, LDA (20.4 mL of a 2.5 M solution, 51.0 mmol) was added dropwise to a solution of 1-hexyluracil (2.0 g, 10.2 mmol) in THF (55 mL), and the resulting solution was stirred under N₂ for 2 h. I₂ (12.9 g, 51.0 mmol) was added and the reaction mixture was stirred for another 2 h at the same temperature. Acetic acid (2.0 mL) was added to react with stirring at room temperature overnight. The organic phase was extracted with ethyl acetate and washed with saturated NaHCO₃ (3 × 30.0 mL) and Na₂SO₃ (3 × 30 mL) solutions. Finally, the product was washed with brine (30 mL) and dried over Mg₂SO₄. The solvent was removed by rotary evaporator and the crude product was purified by column chromatography silica (hexane–ethyl acetate = 5 : 5) to afford compound 9 (2.2 g, 67%). ¹H NMR (300 MHz, CDCl₃): 9.48 (br, 1H), 6.41 (s, 1H), 4.0 (t, *J* = 8.1 Hz, 2H), 1.69–1.64 (m, 2H), 1.37–1.32 (m, 6H), 0.88 (t, *J* = 6.9 Hz, 3H).

Synthesis of 6-(4-bromo-2,5-bis-octyloxy-phenylethynyl)-1-hexyl-1H-pyrimidine-2,4-dione (10). To a mixture of compound 9 (1.26 g, 3.9 mmol) in THF (15 mL), 1-bromo-4-ethynyl-2,5-bis-octyloxy-benzene (6) (2.0 g, 3.9 mmol), CuI (10 mg, 0.05 mmol) and NEt₃ (15 mL) were added. Then, [Pd(PPh₃)₂ Cl₂] (4 mg, 0.034 mmol) was added under N₂ and the reaction mixture was heated to 50 °C for 36 h. The crude product was extracted with DCM followed by brine wash and dried over Mg₂SO₄. The resulting solution was concentrated by rotary evaporator, and purified by column chromatography using silica (hexane–ethyl acetate = 7 : 3) to give a yellow solid. (1.98 g, yield 58%). ¹H NMR (300 MHz, CDCl₃): 9.32 (br, 1H), 7.12 (s, 1H), 6.93 (s, 1H), 5.98 (s, 1H), 4.0 (t, *J* = 6.1 Hz, 2H), 3.96 (t, *J* = 7.5 Hz, 4H), 1.86–1.69 (m, 6H), 1.48–1.27 (m, 26H), 0.88 (t, *J* = 6.9 Hz, 9H); ¹³C NMR (75 MHz, CDCl₃): 162.9, 155.2, 151.0, 149.6, 139.2, 117.7, 117.5, 116.9, 109.1, 106.5, 97.4, 84.8, 70.4, 69.7, 46.8, 32.0, 31.7, 29.5, 29.3, 29.1, 26.5, 26.2, 26.1, 22.9, 22.7, 14.3, 14.2; (FAB) calculated: 630.30; found: 630.30.

Synthesis of 6-(2,5-bis-octyloxy-4-trimethylsilanylethynyl-phenylethynyl)-1-hexyl-1H-pyrimidine-2,4-dione (11). Compound 11 was synthesized as per the synthetic procedure of compound 5 with a final 89% yield; ¹H NMR (300 MHz, CDCl₃): 9.32 (br, 1H), 7.12 (s, 1H), 6.93 (s, 1H), 5.98 (s, 1H), 4.0 (t, *J* = 6.1 Hz, 2H), 3.96 (t, *J* = 7.5 Hz, 4H), 1.86–1.69 (m, 6H), 1.48–1.27 (m, 26H), 0.88 (t, *J* = 6.9 Hz, 9H), 0.12 (s, 9H); ¹³C NMR (75 MHz, CDCl₃): 162.9, 155.2, 151.0, 149.6, 139.2, 117.7, 117.5, 116.9, 109.1, 106.5, 99.3, 99.0, 97.4, 84.8, 70.4, 69.7, 46.8, 32.0, 31.7, 29.5, 29.3, 29.1, 26.5, 26.2, 26.1, 22.9, 22.7, 15.7, 14.3, 14.2, 0.17; (FAB) calculated: 648.43; found: 648.43.

Synthesis of 6-(4-ethynyl-2,5-bis-octyloxy-phenylethynyl)-1-hexyl-1H-pyrimidine-2,4-dione (12). Compound 12 was synthesized as per the synthetic procedure of compound 6 with a final 89% yield; ¹H NMR (300 MHz, CDCl₃): 9.32 (br, 1H), 7.12 (s, 1H), 6.93 (s, 1H), 5.98 (s, 1H), 4.0 (t, *J* = 6.1 Hz, 2H), 3.96 (t, *J* = 7.5 Hz, 4H), 3.31 (s, 1H), 1.84–1.74 (m, 6H), 1.46–1.28 (m, 26H), 0.88 (t, *J* = 6.9 Hz, 9H); ¹³C NMR (75 MHz, CDCl₃): 162.9, 155.2, 151.0, 149.6, 139.2, 117.7, 117.5, 116.9, 109.1, 106.5, 99.3, 99.0, 97.4, 84.8, 81.8, 79.5, 70.4, 69.7, 46.8, 32.0, 31.7, 29.5, 29.3, 29.1, 26.5,

26.2, 26.1, 22.9, 22.8, 14.3, 14.2; (FAB) calculated: 576.39; found: 576.39; elemental analysis; calculated: C, 74.96; H, 9.09; N, 4.86%, found: C, 74.67; H, 9.06, N, 4.88%.

Synthesis of 4-bromo-2,5-bis-octyloxy-benzaldehyde (13). 5 g of compound **6** in 50 mL THF was stirred under N₂ atm and cooled to -78 °C maintained for 1 h. To the solution, 1 equiv. of *n*-BuLi was added, then temperature was raised to 0 °C; 1 equiv. of DMF was added and stirred for 12 h at RT. Excess *n*-BuLi was quenched with two drops of HCl and the solvent was distilled out. Finally, a pure compound was obtained *via* column (SiO₂) 9 : 1 hexane-EtOAc to afford a yellow solid. Yield: 3.03 g (74%); ¹H NMR (300 MHz, CDCl₃): 10.40 (s, 1H), 7.29 (s, 1H), 7.21 (s, 1H), 3.99 (t, *J* = 6.0 Hz, 4H), 1.84–1.74 (m, 4H), 1.46–1.28 (m, 20H), 0.88 (t, *J* = 6.0 Hz, 6H).

Synthesis of 2-(4-bromo-2,5-bis-octyloxy-phenyl)-1H-1,3,7,8-tetraaza-cyclopenta[*l*]-phenanthrene (15). A 1 : 1 mixture of aldehyde (**11**) and phenanthroline diketone (**14**) was dissolved completely in acetic acid. To that solution an excess (30 equiv.) of NH₄OAc was added and refluxed for 12 h. The product formation was monitored by TLC. After completion the crude product was recrystallized from absolute ethanol to afford compound **15** with 94% yield; ¹H NMR (300 MHz, CDCl₃): 11.13 (s, 1H), 9.05 (s, 2H), 8.85 (d, 1H), 7.92 (s, 2H), 7.49–7.60 (m, 2H), 7.07 (s, 1H), 4.08 (t, *J* = 6 Hz, 2H) 3.99 (t, *J* = 6.1 Hz, 2H), 1.84–1.74 (m, 4H), 1.46–1.28 (m, 20H), 0.88 (t, *J* = 6.9 Hz, 6H); ¹³C NMR (75 MHz, CDCl₃): 150.5, 149.8, 148.7, 148.3, 148.2, 135.7, 130.5, 127.9, 124.7, 124.5, 123.3, 122.7, 118.7, 117.8, 117.1, 114.3, 112.7, 70.2, 60.9, 32.1, 29.8, 29.7, 29.6, 29.5, 26.7, 26.3, 22.9, 22.7, 14.4, 14.2; (FAB) calculated: 630.3; found: 630.3; elemental analysis; calculated: C, 66.55; H, 6.86; N, 8.87%, found: C, 66.57; H, 6.81, N, 8.88%.

Synthesis of 2-(4-bromo-2,5-bis-octyloxy-phenyl)-1H-1,3,7,8-tetraaza-cyclopenta[*l*]phenanthrene platinum dichloride (16). A 1 : 1 mixture of compound **15** and PtCl₂(NH₂)₂ was dissolved completely in DMSO and refluxed at 100 °C for 12 h to afford yellow solid of compound **16**. The solid was filtered off and washed with excess water and dried over vacuum at 70 °C for 6 h. Yield: 63%; ¹H NMR (300 MHz, CDCl₃): 11.13 (br, s, 1H), 9.02 (br, s, 2H), 8.78 (br, s, 2H), 8.49 (br, s, 2H), 7.31–7.55 (br, m, 2H), 6.76 (br, s, 1H), 4.08 (br, t, 2H) 3.96 (br, t, 2H), 1.79–1.26 (br, m, 24H), 0.91 (br, t, 6H); (FAB) calculated: 897.63; found: 897.63.

Synthesis of PtC. To a mixture of compound **16** (1 equiv.) in THF (15 mL), 6-(4-ethynyl-2,5-bis-octyloxy-phenylethynyl)-1-hexyl-1H-pyrimidine-2,4-dione (**6**) (10 equiv.), CuI (0.1 equiv.) and NEt₃ (15 mL) were added. Then, PdCl₂(PPh₃)₂ (1 equiv.) was added under N₂ and the reaction mixture was stirred at room temperature for 48 h. The crude product was extracted with DCM followed by brine wash and dried over Mg₂SO₄. The resulting solution was concentrated by rotary evaporator, and purified by column chromatography using neutral alumina (CH₂Cl₂-MeOH = 9 : 1) to give a yellow solid. Yield: 72%; ¹H NMR (300 MHz, CDCl₃): 11.08 (s, 3H(NH)), 7.12 (m, 7H), 6.83 (m, 7H), 6.61 (s, 1H (NH)), 5.98 (s, 3H) 4.09 (t, *J* = 6.1 Hz, 6H), 3.96 (t, *J* = 7.5 Hz, 16H), 1.84–1.74 (m, 24H), 1.46–1.28 (m, 96H), 0.88 (t, *J* = 6.9 Hz, 33H); ¹³C NMR (75 MHz, CDCl₃): 162.5, 155.2, 151.0, 149.6, 139.2, 130.5, 127.8, 124.7, 124.2, 123.3, 122.7, 118.7, 117.7, 117.1, 114.3, 112.7, 109.1, 106.5, 99.3, 99.0, 97.4,

84.8, 81.8, 70.4, 69.7, 46.8, 32.0, 31.7, 29.5, 29.3, 29.1, 26.5, 26.2, 26.1, 22.9, 22.7, 14.3, 14.2; MALDI-TOF; calculated: 2473.24, found: 2473.24; elemental analysis; calculated: C, 69.42; H, 7.98; N, 5.66%, found: C, 68.57; H, 7.76, N, 5.58%.

Acknowledgements

This project was financially supported by the National Science Council of Taiwan (ROC) through funding nos NSC 101-2113-M-009-013-MY2 and NSC 102-2221-E-009-174.

References

- (a) J. M. Lehn, *Supramolecular Chemistry: Concepts and perspectives*, VCH, Weinheim, Germany, 1995; (b) E. C. Constable, in *Comprehensive Supramolecular Chemistry*, ed. J. M. Lehn, Pergamon, Elmsford, NY, 1996, 9, 213.
- (a) J. Jones, *Chem. Soc. Rev.*, 1998, 27, 289; (b) N. Lanigan and X. Wang, *Chem. Commun.*, 2013, 49, 8133.
- (a) F. M. Menger, *Proc. Natl. Acad. Sci. U. S. A.*, 2002, 99, 4818; (b) M. Elhabiri and A.-M. Elberecht-Gary, *Coord. Chem. Rev.*, 2008, 252, 1079; (c) T. F. De Greef, M. M. J. Smulders, M. Wolffs, A. P. H. J. Schenning, R. P. Sijbesma and E. W. Meijer, *Chem. Rev.*, 2009, 109, 5687; (d) X. Wang and R. Mchale, *Macromol. Rapid Commun.*, 2010, 31, 331.
- (a) C. H. Hunag, N. D. McClenaghan, A. Kuhn, J. W. Hotstraat and D. M. Bassani, *Org. Lett.*, 2005, 7, 3409; (b) D. M. Bassani, L. Jonuusaukaite, A. Lavie-Cambot, N. D. McClennaghan, J. L. Pozzo, D. Ray and G. Vives, *Coord. Chem. Rev.*, 2010, 254, 2429.
- (a) U. S. Schubert and M. Heller, *Chem.-Eur. J.*, 2001, 7, 5253; (b) K. S. Mali, K. Lava, K. Binnemans and S. D. Feyter, *Chem.-Eur. J.*, 2010, 16, 14447.
- (a) L. J. Prins, D. N. Reinhoudt and P. Timmerman, *Angew. Chem., Int. Ed.*, 2001, 40, 2382; (b) M. J. Weister, P. A. Ulmann and C. A. Mirkin, *Angew. Chem., Int. Ed.*, 2011, 50, 114; (c) A. Das and S. Ghosh, *Angew. Chem., Int. Ed.*, 2014, 53, 2038.
- (a) K. L. Hass and K. J. Franz, *Chem. Rev.*, 2009, 109, 4921; (b) M. Wegner, D. Dudenko, D. Sebastiani, A. R. A. Palmans, T. F. A. de Greef, D. Graf and H. W. Spiess, *Chem. Sci.*, 2011, 2, 2040; (c) T. C. Liang and H. C. Lin, *J. Mater. Chem.*, 2009, 19, 4753; (d) B. K. Kuila and M. Stamm, *J. Mater. Chem.*, 2011, 21, 14127; (e) S. A. Gopalan, G. Anantha-Iyengar, B. Han, S. W. Lee, D. H. Kwon, S. H. Lee and S. W. Kang, *J. Mater. Chem. A*, 2014, 2, 2174.
- (a) B. J. Holliday and C. A. Mirkin, *Angew. Chem., Int. Ed.*, 2001, 40, 2022; (b) Y. R. Zheng, Z. Zhao, M. Wang, K. Ghosh, J. Bryant Pollock, T. R. Cook and P. J. Stang, *J. Am. Chem. Soc.*, 2010, 132, 16873; (c) C. Po, A. Y. Y. Tam, K. M. C. Wang and V. W. W. Yam, *J. Am. Chem. Soc.*, 2011, 133, 12136.
- J. Anastassopoulou and T. Theophanides, *NATO ASI Ser., Ser. C*, 1995, 459, 209.
- J. Ribas Gispert, *Coordination Chemistry*, Wiley-VCH, Weinheim, 1st edn, 2008.

- 11 (a) J. M. Lehn, *Science*, 2002, **295**, 2400; (b) G. Cooke and V. M. Rotello, *Chem. Soc. Rev.*, 2002, **31**, 275; (c) Special issue on "Supramolecular Chemistry Anniversary", *Chem. Soc. Rev.*, 2007, **36**, 125; (d) A. L. Pallas, M. Matena, T. Jung, M. Prato, M. Stohr and D. Bonifazi, *Angew. Chem., Int. Ed.*, 2008, **47**, 7726.
- 12 (a) M. D. Ward and P. R. Raithby, *Chem. Soc. Rev.*, 2013, **42**, 1619; (b) D. C. Sherrington and K. A. Taskinen, *Chem. Soc. Rev.*, 2001, **30**, 83; (c) B. M. Schulze, N. T. Shewmon, J. Zhang, D. L. Watkins, J. P. Mudrick, W. Cao, R. B. Zerdan, A. J. Quartararo, I. Ghiviriga, J. Xue and R. K. Castellano, *J. Mater. Chem. A*, 2014, **2**, 1541; (d) A. Besette and G. S. Hanan, *Chem. Soc. Rev.*, 2014, **43**, 3342; (e) W.-Y. Wong and C.-L. Ho, *J. Mater. Chem.*, 2009, **19**, 4457; (f) W.-Y. Wong and C.-L. Ho, *Coord. Chem. Rev.*, 2009, **253**, 1709; (g) G. Zhou, W.-Y. Wong, S.-Y. Poon, C. Ye and Z. Lin, *Adv. Funct. Mater.*, 2009, **19**, 531; (h) W. Y. Wong, X. Z. Wang, Z. He, K. K. Chan, A. B. Djurisic, K. Y. Cheung, C. T. Yip, A. M. Ng, Y. Y. Xi, C. S. K. Mac and W. K. Chan, *J. Am. Chem. Soc.*, 2007, **129**, 14372.
- 13 (a) M. A. Pitt and D. W. Johnson, *Chem. Soc. Rev.*, 2007, **36**, 1441.
- 14 (a) A. V. Klein and T. W. Hambley, *Chem. Rev.*, 2009, **109**, 4911; (b) J. Z. Zhang, P. Bonnitca, E. Wexselblatt, A. V. Klein, Y. Najajreh, D. Gibson and T. W. Hambley, *Chem.-Eur. J.*, 2012, **19**, 1672; (c) X. Wang and Z. Guo, *Chem. Soc. Rev.*, 2013, **42**, 202.
- 15 L. Kelland, *Nat. Rev. Cancer*, 2007, **7**, 573.
- 16 L. B. Xing, S. Yu, X. J. Wang, G. X. Wang, B. Chen, L. P. Zhang, C. H. Tung and L. Z. Wu, *Chem. Commun.*, 2012, **48**, 10886.
- 17 M. Shirakawa, N. Fujita, T. Tani, K. Kaneko and S. Shinkai, *Chem. Commun.*, 2005, 4149.
- 18 (a) A.-M. Caminade and J.-P. Majoral, *Chem. Soc. Rev.*, 2010, **39**, 2034; (b) S. C. Lo and P. L. Burn, *Chem. Rev.*, 2007, **107**, 1097; (c) U. D. Astruc, E. Boisselier and C. Ornelas, *Chem. Soc. Rev.*, 2010, **110**, 1857; (d) B. Romagnoli and W. Hayes, *J. Mater. Chem.*, 2002, **12**, 767.
- 19 (a) K. V. Rao, K. K. R. Datta, M. Eswaramoorthy and S. J. George, *Chem.-Eur. J.*, 2012, **18**, 2184; (b) K. Ariga, H. Ito, J. P. Hill and H. Tsukube, *Chem. Soc. Rev.*, 2012, **41**, 5800; (c) J. Khandare, M. Calderón, N. M. Dagia and R. Haag, *Chem. Soc. Rev.*, 2012, **41**, 2824; (d) J. Satija, V. V. R. Sai and S. Mukherji, *J. Mater. Chem.*, 2011, **21**, 14367; (e) G. M. Soliman, A. Sharma, D. Maysinger and A. Kakkar, *Chem. Commun.*, 2011, **47**, 9572; (f) F. C. De Schryver, T. Vosch, M. Cotlet, M. V. Auweraer, K. Mollen and J. Hofkens, *Acc. Chem. Res.*, 2005, **38**, 514.
- 20 Y. Song, Y. Yang, C. J. Medforth, E. Pereira, A. K. Singh, H. Xu, Y. Jiang, J. Brinker, F. V. Swol and J. A. Shelnutt, *J. Am. Chem. Soc.*, 2004, **126**, 635.
- 21 (a) K. E. Sapsford, L. Berti and I. L. Medintz, *Angew. Chem., Int. Ed.*, 2006, **45**, 4562; (b) Q. Zhao, F. Li and C. Huang, *Chem. Soc. Rev.*, 2010, **39**, 3007; (c) J. Liu, W. He and Z. Guo, *Chem. Soc. Rev.*, 2013, **42**, 1568; (d) C. Qin, W.-Y. Wong and L. Wang, *Macromolecules*, 2011, **44**, 483; (e) X. Yang, Z. Huang, J. Dang, C.-L. Ho, G. Zhou and W.-Y. Wong, *Chem. Commun.*, 2013, **49**, 4406; (f) X. Yang, Z. Huang, C.-L. Ho, G. Zhou, D. R. Whang, C. Yao, X. Xu, S. Y. Park, C.-H. Chui and W.-Y. Wong, *RSC Adv.*, 2013, **3**, 6553.
- 22 X. Zhang, Z. Han, Z. Fang, G. Shen and R. Yu, *Anal. Chim. Acta*, 2006, **562**, 210.
- 23 S. Silver, *FEMS Microbiol. Rev.*, 2003, **27**, 341.
- 24 (a) J. F. Zhang, Y. Zhou, J. J. Yoon and J. S. Kim, *Chem. Soc. Rev.*, 2011, **40**, 3416; (b) T. Pradhan, H. S. Jung, J. H. Jang, T. W. Kim, C. Kang and J. S. Kim, *Chem. Soc. Rev.*, 2014, **43**, 4684; (c) Z. Yang, J. Cao, Y. He, J. H. Yang, T. Kim, X. Peng and J. S. Kim, *Chem. Soc. Rev.*, 2014, **43**, 4563; (d) R. Kumar, Y. O. Lee, V. Bhalla, M. Kumar and J. S. Kim, *Chem. Soc. Rev.*, 2014, **43**, 4824.
- 25 (a) E. Bielli, R. D. Gillard and D. W. James, *J. Chem. Soc., Dalton Trans.*, 1976, 1837; (b) T. J. Wadas, R. J. Lachichotte and R. Eisenberg, *Inorg. Chem.*, 2003, **42**, 3772.
- 26 (a) H. Padhy, D. Sahu, I.-H. Chiang, D. Patra, D. Kekuda, C.-W. Chu and H.-C. Lin, *J. Mater. Chem.*, 2011, **21**, 1196; (b) W.-S. Huang, Y.-H. Wu, H.-C. Lin and J. T. Lin, *Polym. Chem.*, 2010, **1**, 494; (c) C. W. Wu and H. C. Lin, *Macromolecules*, 2006, **39**, 7985.
- 27 (a) S. Muthaiah, Y. C. Rajan and H. C. Lin, *J. Mater. Chem.*, 2012, **22**, 8976; (b) Y. C. Rajan, S. Muthaiah, C. T. Huang, H. C. Lin and H. C. Lin, *Tetrahedron*, 2012, **68**, 7926.
- 28 (a) S. Yagai, M. Higashi, T. Kinoshita, K. Kishikawa, T. Nakanshi, T. Karatsu and A. Kitamura, *J. Am. Chem. Soc.*, 2007, **129**, 13277; (b) T. E. Kaiser, V. Stepanenko and F. Wurthner, *J. Am. Chem. Soc.*, 2009, **131**, 6719.
- 29 (a) Y. Liu, J. Zhuang, H. Liu, Y. Li, F. Lu, H. Gan, T. Jiu, N. Wang, X. He and D. Zhu, *Chem. Phys. Chem.*, 2004, **5**, 1210; (b) Y. Liu, J. Zhuang, H. Liu, Y. Li, F. Lu, H. Gan, T. Jiu, N. Wang, X. He and D. Zhu, *J. Org. Chem.*, 2004, **69**, 9049; (c) X. Xiao, W. Xu, D. Zhang, H. Xu, H. Lu and D. Zhu, *J. Mater. Chem.*, 2005, **15**, 2557.
- 30 A. P. H. J. Schunning, J. V. Jonkheijm, Z. Chen, F. Wurthner and E. W. Meijer, *J. Am. Chem. Soc.*, 2002, **124**, 10252.
- 31 (a) D. V. Kozlov, D. S. Tyson, C. Goze, R. Ziessel and F. N. Castellano, *Inorg. Chem.*, 2004, **43**, 6083; (b) D. S. Tyson, C. R. Luman, X. Zhou and F. N. Castellano, *Inorg. Chem.*, 2001, **40**, 4063.
- 32 B. Ventura, A. Barbieri, F. Barigelletti, S. Diring and R. Ziessel, *Inorg. Chem.*, 2010, **49**, 8333.
- 33 (a) D. Bradshaw, A. Garai and J. Huo, *Chem. Soc. Rev.*, 2012, **41**, 2344; (b) D. C. Sherrington and K. A. Taskinen, *Chem. Soc. Rev.*, 2001, **30**, 83.
- 34 M. L. Yu, S. M. Wang, K. Feng, T. Khoury, M. J. Crossley, Y. Fan, J. P. Zhang, C. H. Tung and L. Z. Wu, *J. Phys. Chem. C*, 2011, **115**, 23634.
- 35 K. Adachi, Y. Sugiyama, K. Yoneda, K. Yamada, K. Nozaki, A. Fuyuhira and S. Kawata, *Chem.-Eur. J.*, 2005, **11**, 6616.
- 36 (a) H. C. Chu, Y. H. Lee, S. J. Hsu, P. J. Yang, A. Yabushita and H. C. Lin, *J. Phys. Chem. B*, 2011, **115**, 8845; (b) P. J. Yang, H. C. Chu, T. C. Chen and H. C. Lin, *J. Mater. Chem.*, 2012, **22**, 12358.
- 37 (a) Y. Wang, D. Zhou, H. Li, R. Li, Y. Zhong, X. Sun and X. Sun, *J. Mater. Chem. C*, 2014, **2**, 6402; (b) H. Kar,

- M. R. Molla and S. Ghosh, *Chem. Commun.*, 2013, **49**, 4220; (c) F. F. Camerel, R. Ziessel, B. Donnio, C. Bourgogne, D. Guillon, M. Schmutz and C. Lacovita, *Angew. Chem., Int. Ed.*, 2007, **119**, 2713; (d) O. M. Yaghi, H. Li and T. L. Groy, *J. Am. Chem. Soc.*, 1996, **118**, 9096.
- 38 (a) N. Niamnont, N. Kimpitak, K. Wongravee, P. Rashatasakhon, K. K. Baldrige, J. S. Siegel and M. Sukwattanasinitt, *Chem. Commun.*, 2013, **49**, 780; (b) S. Sirilaksanapong, M. Sukwattanasinitt and P. Rashatasakhon, *Chem. Commun.*, 2012, **48**, 293; (c) N. Niamnont, W. Siripornnoppakhun, P. Rashatasakhon and M. Sukwattanasinitt, *Org. Lett.*, 2009, **11**, 2768.
- 39 (a) S. Muthaiah, Y. H. Wu and H. C. Lin, *Analyst*, 2013, **138**, 2931; (b) S. Muthaiah, Y. H. Wu, A. Singh, M. V. R. Raju and H. C. Lin, *J. Mater. Chem. A*, 2013, **1**, 1310; (c) H. P. Fang, S. Muthaiah, A. Singh, M. V. R. Raju, Y. H. Wu and H. C. Lin, *Sens. Actuators, B*, 2014, **194**, 229.